Knockdown of the glucocorticoid receptor alters functional integration of newborn neurons in the adult hippocampus and impairs fear-motivated behavior

Fitzsimons, C.P.; Hooijdonk, L.W.A. van; Schouten, M.; Zalachoras, I.; Brinks, V.; Zheng, T.; ... ; Vreugdenhil, E.

npg

ORIGINAL ARTICLE

Knockdown of the glucocorticoid receptor alters functional integration of newborn neurons in the adult hippocampus and impairs fear-motivated behavior

CP Fitzsimons[1,2,8], LWA van Hooijdonk[1,8], M Schouten[2], I Zalachoras[1], V Brinks[1], T Zheng[3], TG Schouten[1], DJ Saaltink[1], T Dijkmans[1], DA Steindler[3], J Verhaagen[4], FJ Verbeek[5], PJ Lucassen[2], ER de Kloet[1], OC Meijer[1], H Karst[6], M Joels[6], MS Oitzl[1] and E Vreugdenhil[1,7]

Glucocorticoids (GCs) secreted after stress reduce adult hippocampal neurogenesis, a process that has been implicated in cognitive aspects of psychopathology, amongst others. Yet, the exact role of the GC receptor (GR), a key mediator of GC action, in regulating adult neurogenesis is largely unknown. Here, we show that GR knockdown, selectively in newborn cells of the hippocampal neurogenic niche, accelerates their neuronal differentiation and migration. Strikingly, GR knockdown induced ectopic positioning of a subset of the new granule cells, altered their dendritic complexity and increased their number of mature dendritic spines and mossy fiber boutons. Consistent with the increase in synaptic contacts, cells with GR knockdown exhibit increased basal excitability parallel to impaired contextual freezing during fear conditioning. Together, our data demonstrate a key role for the GR in newborn hippocampal cells in mediating their synaptic connectivity and structural as well as functional integration into mature hippocampal circuits involved in fear memory consolidation.

INTRODUCTION

In the adult brain, neural progenitor cells (NPCs) exist in the subgranular cell layer (GCL) of the dentate gyrus (DG), a subfield of the hippocampus involved in learning and memory formation.[1] NPCs generate proliferative neuroblasts that migrate and eventually differentiate into fully functional granule neurons. The adult-born cells become well integrated into the existing hippocampal network,[2] a process known as adult neurogenesis, in approximately 5 weeks.[3] Previous studies using pharmacological, physical or genetic ablation strategies have implicated adult neurogenesis in hippocampus-dependent cognitive functions, amongst others.[4]

Glucocorticoids (GCs) are important mediators of the stress response that are among the best-studied negative regulators of neurogenesis.[1,5,6] Exposure to both acute or chronic stress, as well as to chronic GC administration, reduces the numbers of newborn neurons or their survival.[5,7,8] In contrast, removal of endogenous GCs by adrenalectomy stimulates neurogenesis.[5] Paradoxically, voluntary exercise, enriched environment and certain learning paradigms stimulate neurogenesis even though they elevate endogenous GC levels as well.[9,10] Stress and GCs can further enhance the memory of stress-related events by a GC receptor (GR)-mediated signaling cascade.[11,12] Together, these data raise the question whether the effects of GCs on adult neurogenesis

occur directly or in an indirect manner, for example, through GC-induced *N*-methyl-D-aspartic acid receptor activation.[13]

GCs generally exert their effects by binding to two types of receptors, the GRs and the mineralocorticoid receptors (MRs). Both MRs and GRs act as transcription factors that, upon GC binding, translocate to the nucleus where they activate specific target genes through transactivation or transrepression.[14] Several studies implicate GR involvement in neurogenesis regulation. Thus, prolonged periods of GR activation, induced by, for example, chronic stress, decrease levels of neurogenesis,[6,15] whereas brief treatments with the GR antagonist mifepristone, for example, normalize both the chronic corticosterone or chronic stress-induced reductions in neurogenesis,[7,8,16] suggesting direct involvement of GRs in the regulation of neurogenesis.

In the brain, activated MRs and GRs exert profound genomic effects on the hippocampal networks that underlie behavioral adaptation to stress, a concept that may be involved in several brain diseases. For instance, chronic stress has been implicated in the memory impairments and cognitive decline common to several psychiatric disorders.[17] Numerous studies in humans further suggest that aberrant GR signaling represents a risk factor for depression[18] and that normalization of GR signaling precedes the clinical responses to antidepressant therapies.[18] In

[1]Department of Medical Pharmacology, Leiden University Medical Center/Leiden Amsterdam Center for Drug Research, Leiden, The Netherlands; [2]Center for Neuroscience, Swammerdam Institute for Life Sciences, University of Amsterdam, Amsterdam, The Netherlands; [3]Department of Neurosurgery, College of Medicine, McKnight Brain Institute, University of Florida, Gainesville, FL, USA; [4]Laboratory for Neuroregeneration, Netherlands Institute for Neuroscience, Royal Academy of Arts and Sciences, Amsterdam, The Netherlands; [5]Leiden Institute for Advanced Computer Sciences (LIACS), Leiden University, Leiden, The Netherlands; [6]Division Neuroscience, Rudolf Magnus Institute, UMC, Utrecht, The Netherlands and [7]Department of Human Genetics, Migraine Research Group, Leiden University Medical Centre, Leiden, The Netherlands. Correspondence: Dr E Vreugdenhil, Department of Human Genetics, Migraine Research Group, Leiden University Medical Centre, Einthovenweg 20, Building 2, Room T3-52, Postzone S4-P; PO Box 9600, Leiden 2300RC, The Netherlands.
E-mail: e.vreugdenhil.HG@lumc.nl
[8]These authors contributed equally to this work.
Received 13 February 2011; revised 28 June 2012; accepted 5 July 2012; published online 28 August 2012

line with these data, transgenic mice with impaired GR signaling exhibit not only behavioral similarities to human depression but also show altered levels of hippocampal neurogenesis.[19,20]

Despite the wealth of information on the effect of stress and GCs on neurogenesis, very little is known about the exact role of GRs in the adult hippocampal neurogenic niche. Reverse-transcription PCR experiments indicate that GR, but not MR, is expressed in cultured adult DG-derived NPCs.[21] More detailed immunohistochemical evidence indicates that GR, but not MR, is expressed in 50% of all subpopulations of proliferative progenitor cells, except for some neuroblasts of the type 2b, which do not express GRs or MRs.[22] Together, these studies suggest a direct role for GRs, but not MRs, in a subpopulation of adult NPCs in the DG. Two recent studies further suggest that a tight control of GRs in NPCs is necessary to regulate neurogenesis. First, doublecortin (DCX)-like, a microtubule-associated protein that is specifically expressed in NPCs and is closely related to DCX,[23] regulates the transport of activated GRs to the nucleus, suggesting that NPCs contain specific mechanisms to regulate GR activity.[24] Second, miR-124a, a microRNA that regulates neuronal differentiation of NPCs in vivo,[25] also controls GR expression at the protein level and regulates GR activity in NPCs.[26] Yet, it is entirely unknown how the development of the adult NPCs themselves is affected by changes in their endogenous level of GR expression.

In the present study, we therefore tested the hypothesis that the morphology and positioning of NPCs in the GCL, as well as their functional contribution to the hippocampal circuitry, critically depends on GR-mediated GC signaling in the NPCs themselves. Here we targeted GRs, selectively in the newborn cells, using viral-mediated RNA-interference in the hippocampus in vivo. Selective GR knockdown in the newborn cells resulted in their accelerated migration through GCL and an ectopic positioning in the GCL, an aberrant developmental pattern that was associated with an increased excitability of the newborn cells, as well as with impairments in memory consolidation studied in the hippocampus in vivo.

MATERIALS AND METHODS
Methods are described in more detail in 'Supplementary Methods'.

Animals
Upon arrival, male BALB/c mice (6 weeks old, Janvier Bioservices, Genest st Isle, France) were individually housed for 1 week in filtertop cages before stereotaxic surgery. Mice had free access to food and water, and were kept under a 12-h dark/light cycle (lights on at 0800 h) in a temperature- (20 °C) and humidity-controlled room. All lentiviral experiments were approved by the committee on Animal Health and Care from the Leiden University, and all retroviral experiments were approved by the committee on Animal Health and Care from the Netherlands Institute for Neuroscience (NIM; DEC protocol NIN 1180). All animal experiments were performed under guidelines of the Netherlands Ministry of Health for the use of genetically modified organisms and were executed in strict compliance with the European Union recommendations for the care and use of laboratory animals.

Lentiviral vectors
To produce the lentiviruses LV-PM (perfect match) and LV-MM (mismatch), effective short-hairpin RNA (shRNA) against the GR (shGR2) and its corresponding mismatched control shGR2m were subcloned into replication-incompetent and self-inactivating advanced generation lentiviral vectors (pLV-CMV-eGFP), respectively. LVs were produced and titrated as previously described.[24] Titers of both viruses were comparable and ranged between 1×10^8 and 1×10^9 transducing U ml^{-1}. Virus suspensions were stored at -80 °C until use, and were briefly centrifuged and kept on ice immediately before injection.

Stereotaxic surgery
Stereotaxic injections were performed in the morning, according to previously described methods.[27] All animals were injected bilaterally into

the hilus of the DG (anterior-posterior: -2.00 mm, molecular layer: ± 1.50 mm, dorsal-ventral: -1.90 mm, relative to Bregma), with an injection volume of 1 μl (virus titer $= 1 \times 10^8$ transducing U μl^{-1}, rate $= 0.4$ ml min^{-1}). For fear-conditioning experiments, animals were injected with shGR2 ($N = 40$ animals) or shGR2m constructs ($N = 40$ animals), and tested 5 weeks post surgery. For immunocytochemistry, a group of 40 mice ($N = 20$ for shGR2 and $N = 20$ for shGR2m) was injected and killed 1 week post surgery ($N = 10$ for shGR2 and $N = 10$ for shGR2m) or 5 weeks post surgery ($N = 10$ for shGR2 and $N = 10$ for shGR2m). For electrophysiological experiments, 20 mice were injected and killed 5 weeks post surgery ($N = 10$ LV-PM and $N = 10$ LV-MM). In all experiments, mice were only included for analysis when postmortem histological evidence was present of an appropriately targeted microinjection, as visualized by enhanced green fluorescent protein (EGFP) expression. For retroviral transduction, 20 animals were injected with retroviruses expressing RVhairpin0, RVhairpin2, RVhairpinLNK and RVhairpinSCRB (Supplementary Methods section), 5 animals per group. Retrovirus-injected animals were killed 14 days after the injection, transcardially perfused with freshly prepared 4% paraformaldehyde and further processed for immunofluorescence staining for GFP using a recombinant rabbit monoclonal anti-GFP antibody (1:200; Invitrogen, Bleiswijk, The Netherlands).

Immunohistochemistry
Tissue preparation, sectioning and immunocytochemical staining for cell-type-specific markers and their quantification was done as described.[27,28] Samples in which primary antibodies were excluded were processed in parallel and used as negative controls.

Confocal microscopy and image analysis
One or five weeks after injection, animals were killed and brains were fixed by transcardial perfusion. Brains were extracted, sectioned and immuno-stained as described before.[28] Confocal microscopy experiments were performed using a Digital Eclipse C1si spectral confocal laser fluorescence microscope system (Nikon, Amstelveen, The Netherlands). From the confocal images, quantification of EGFP + cells and quantitative analysis of different classes of neuronal cells indicated by expression of cell-type-specific markers were performed using the optical fractionator sampling method and a previously validated semi-automated method based on Cell Profiler software, as recently described.[24,27] Sections surrounding the injection site were discarded. The GCL was subdivided in four 2-cell-body-wide sublayers denominated subgranular zone (SGZ) and GCL 1 to 3 (Supplementary Figure 5). In all cases, a minimum of 100 cells was analyzed of randomly selected sections across the dorsoventral axis of the hippocampus per animal of each experimental group ($N = 5$ animals). A few cells present in the apex of the DG were excluded because of difficulties to reproducibly assign them to distinct GCL sublayers.

Dendritic spine three-dimensional reconstructions and shape classifications
Three-dimensional reconstruction of dendritic segments was done from Z-stacks of confocal images series of 100–200 confocal planes taken at 0.1-μm intervals using a $\times 63$ oil immersion objective and a digital zoom factor of 4. The confocal stacks were then deconvolved with Huygens Deconvolution Software (Scientific Volume Imaging b.v, Hilversum, The Netherlands). Spine density and morphology reconstructions and analysis were performed by automated three-dimensional detection and shape classification based on a Rayburst sampling algorithm and morphology criteria described by Rodriguez et al.,[29] using NeuronStudio (http://www.mssm.edu/cnic/tools-ns.html). Data shown are from 10 dendritic segments for each experimental group ($N = 5$ animals) of an average length of 145 μm each (average spine density 183 spines per segment) and from randomly selected granule cells across the dorsoventral axis of the hippocampus.

Confocal analysis of mossy fiber boutons
Giant mossy fiber boutons in the CA3 area were analyzed as described by others.[30] Z-stacks of confocal images series of 100–200 confocal planes were acquired at 0.75-μm intervals with $\times 40$ oil lens (numerical aperture 1.3; Nikon, Amstelveen, The Netherlands) and a digital zoom of 6. Confocal stacks were then deconvolved using Huygens Deconvolution Software. Data shown are from 150 boutons per experimental group ($n = 5$ animals) from randomly selected sections across the dorsoventral axis of the hippocampus where mossy fibers were visible.

Electrophysiology

In acute hippocampal slices (5 weeks after injection), EGFP + and EGFP − granule cells of both LV-PM and LV-MM groups were assessed for their physiological properties. Using patch clamp techniques, spontaneous miniature excitatory postsynaptic currents (mEPSCs) were recorded as a measure of the spontaneous glutamate-mediated synaptic events (see for detail Supplementary Methods). Recordings of mEPSCs were performed as previously described.[31]

Fear conditioning

Fear conditioning and behavioral assessment of GR knockdown and control mice were performed as previously described.[32] Video-recorded behavior was analyzed by an experimenter unaware of the treatment of the animal. Results are presented as mean ± s.e.m. of each experimental group. For details, see Supplementary Methods.

Corticosterone radioimmunoassay

Corticosterone concentrations were measured in blood plasma using a commercially available radioimmunoassay kit (ICN Biomedicals, Costa Mesa, CA, USA), as described before.[32]

Statistical analysis

All comparisons of GR knockdown animals with control animals were statistically tested using unpaired Student's t-test. When more than two groups were compared, we used one-way analysis of variance test with Tukey's post test if $P < 0.05$, as described before.[27]

RESULTS

Effects of GR knockdown in vitro and in vivo

To better understand the role of GRs in the cells of the adult hippocampus neurogenic niche, we have selectively downregulated GR protein levels in newborn cells using perfect match GR-targeting shRNAs. To control for possible off-target effects, we have generated nearly identical, mismatch control shRNAs, which differed only in two nucleotides from the perfect match (Supplementary Figures 1 and 2, and Supplementary Table S1). These shRNAs were cloned in a previously described LV-based vector[24,27] that was optimized to co-express shRNAs and the EGFP in vivo. Both in (undifferentiated) PC12 cells and after stereotactic injection of LV vectors to the DG in vivo, we observed substantial knockdown of endogenous GRs by the perfect match shRNA (GR knockdown), but not by its mismatch shRNA (control; Supplementary Figures 1 and 2). LV vectors effectively targeted the inner layers of the adult DG, with EGFP expression spanning from anterior (dorsal) to posterior (ventral) areas (see van Hooijdonk et al.[27] and Supplementary Figure 3).

In line with our previous study,[27] 1 week after injection, the majority of the transduced cells were positive for DCX, a well-accepted marker for neurogenesis in the adult brain that is expressed in young, migratory neurons, where it is expressed for 4–14 days after the birth of a new cell until it differentiates into an adult neuron.[33] The morphology of EGFP +/DCX + cells varied from small cells with short or non-existing horizontal processes to cells with long radial processes (Supplementary Figure 4). A small minority of the transduced cells were positive for glial fibrillary acidic protein and nestin, which mark other maturation stages of newborn cells, as previously described.[27] Consistent with the large degree of DCX double positivity of EGFP + cells, newborn neuron labeling with the proliferation marker bromodeoxyuridine (BrdU) yielded EGFP +/BrdU + cells in the GCL, 1 week after LV injection (Supplementary Figure 2). A minority (7%, Supplementary Figure 3) of the cells were located in the hilus and may represent astrocytes or hilar interneurons. Together with our previous results,[27] these observations indicate that in the hippocampal neurogenic niche, our LV has preferentially targeted newborn cells.

We analyzed in more detail the cell type(s) expressing GR in the DG by GR/NeuN and GR/DCX double-labeling. The GR and the mature neuron marker neuronal nuclei antigen (NeuN) were abundantly co-expressed in the DG (Figure 1a). However, in SGZ, GR + cells were found to be in some cases with NeuN + (Figure 1b) and in some others negative for NeuN (Figure 1c). GR + cells in the SGZ were in many cases DCX + (Figure 1d). In line with previous reported type 3 progenitor cells,[22] GR +/DCX + cells were small, with no or very short horizontal processes (Figures 1e and f) and were negative for nestin (not shown).

After lentiviral delivery, GR immunohistochemistry and subsequent semiquantification in EGFP + cells confirmed considerable GR knockdown in vivo, whereas the mismatch control did not affect GR expression (Supplementary Figure 1). To control for possible knockdown of the structurally related MR, we checked MR expression both in vitro and in vivo (Supplementary Figure 1). In agreement with previous studies,[21,22] MR expression was restricted to all cells of the GCL, whereas in the SGZ, it was below detection level. In vivo and in vitro, we did not detect any significant differences in MR expression in EGFP + cells of control versus GR knockdown groups (Supplementary Figure 1), indicating a high target specificity of our perfect-match shRNA.

GR knockdown lead to accelerated neuronal differentiation of newborn granule cells

GCs affect the fate of NPCs in the adult brain,[34] but may do so via activation of GR in NPCs or in other cells in the environment. Here, we investigated the effects of GR knockdown specifically in NPCs. To label proliferating cells, we used both a single injection and daily injections of BrdU during 5 consecutive days. When comparing GR knockdown animals with control animals, we found no significant differences in the number of BrdU cells between control and GR knockdown (Supplementary Figure 2). As indirect effects of GR knockdown may also have a role in the regulation of neurogenesis by GCs,[35] we next developed mouse hippocampus neural stem cell (NSC) cultures (Supplementary Figure 6 and Supplementary Methods section) to further characterize the direct effects of GCs and of GR knockdown on NSCs. Similar to the results obtained with human NSCs,[36,37] long-term incubation of mouse NSCs with the specific GR agonist dexamethasone (DEX) resulted in a significant reduction in cell proliferation as detected by a reduced expression of the proliferation marker Ki67 (Figures 1i–k).

Interestingly, and in contrast to previous observations with higher DEX concentrations,[7] but similar to what has been observed in other cell types,[38] DEX induced a dose-dependent inhibition of caspase-3 activity in mouse NSCs (Figure 1l). This inhibition of caspase-3 activity was significantly reduced by GR knockdown in a magnitude that was proportional to the reduction in GR mRNA induced by specific small interfering RNAs (Figures 1m and n). Moreover, pre-incubation with 1×10^{-7} M DEX significantly reduced both the levels of caspase-3 activity and the number of cells expressing cleaved caspase-3 that was induced by 1×10^{-7} M staurosporine (STS; Supplementary Figure 7 and Supplementary Methods section). Although caspase-3 activation is frequently associated with induction of apoptosis, it is commonly known that activated caspase-3 is also elevated in non-apoptotic, differentiating NSCs,[39] suggesting that neuronal differentiation of NSCs depends on both endogenous caspase-3 activity as well as concentration. Similarly, we observed that STS, a strong inducer of caspase 3 activity[40] exerted dual effects on mouse NSCs. At lower doses, STS reduced caspase-3 activity levels, parallel to neurite thinning and extension. At higher doses, however, STS induced higher caspase-3 activity levels that were associated with neurite collapse, cellular rounding and apoptosis. Interestingly, pre-incubation with 1×10^{-7} M DEX significantly reduced the neurite extension induced by 1×10^{-7} M STS (Supplementary Figure 7). Overall, these results suggest that GR is involved in inhibition of cell proliferation and in
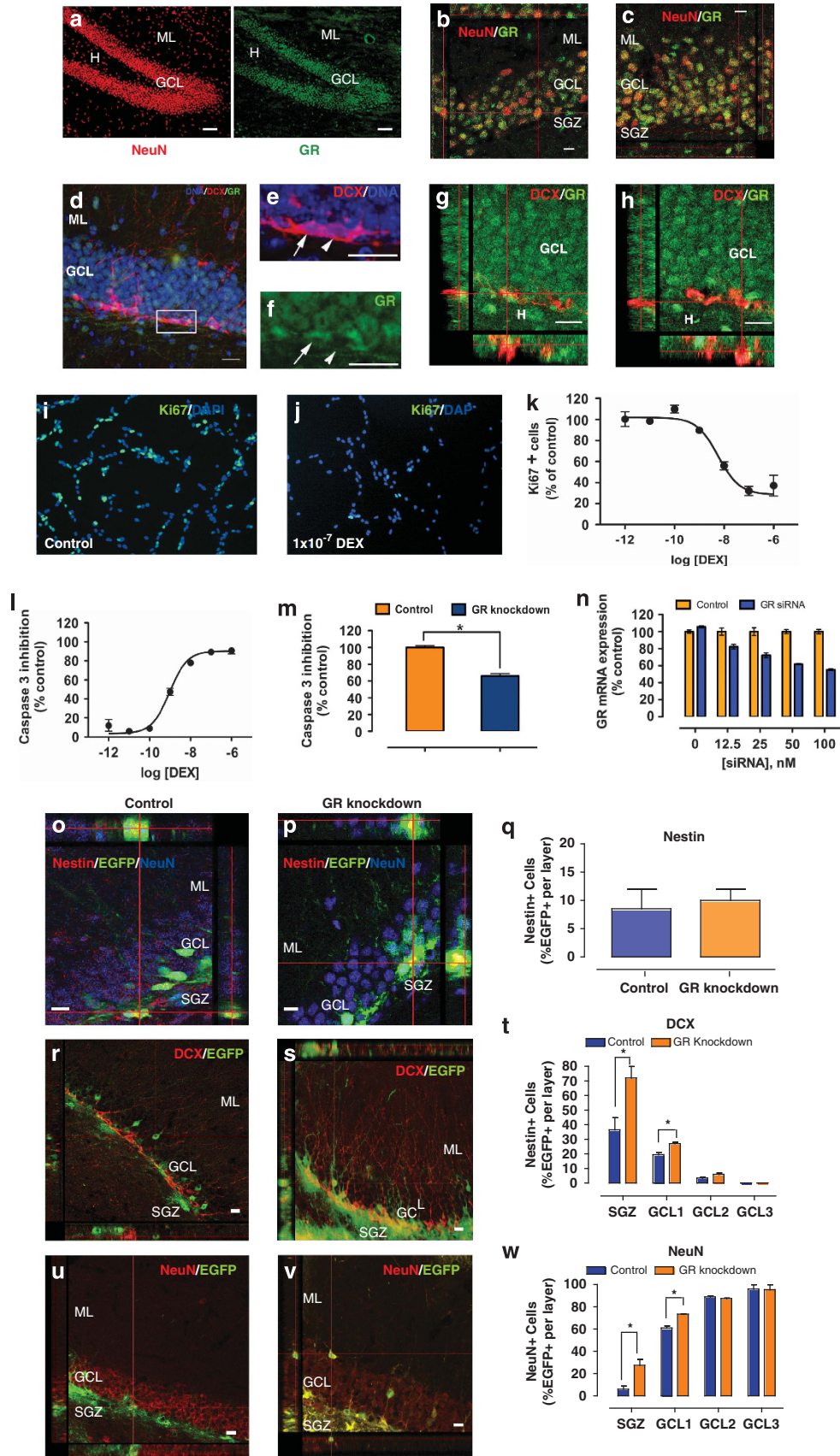
neurite extension, which represent two of the first cellular changes associated with neuronal differentiation,[41] possibly by a caspase 3-dependent mechanism. To study the fate of NSCs and their progeny after GR knockdown in vivo, we next analyzed the expression of three markers of different stages of cell maturation: nestin, DCX and NeuN.

The proportion of EGFP + /nestin$^+$ cells located exclusively in the SGZ layer in both experimental groups, was unaffected by GR knockdown (Figures 1o–q). In contrast, when we analyzed EGFP + cells within the SGZ and in subdivisions of the GCL termed GCL1-3, that is, from the hilus to the molecular layer (see refs 42–44 and Supplementary Figure 5) 1 week after lentiviral injection, we found a significant increase in the proportion of EGFP + cells that were double-labeled for DCX within the SGZ and GCL1 in the GR knockdown animals, as compared with the control mice (Figures 1r–t and Supplementary Figure 8). This was accompanied by a concomitant increase in the proportion of EGFP + cells double-positive for NeuN in the same layers (Figures 1u–w and Supplementary Figure 8). Together, our results strongly suggest that GR knockdown inhibits proliferation and neurite extension, and accelerates maturation of NPCs in the mouse DG.

GR knockdown changes the migration pattern of newborn granule cells in the DG

During neuronal differentiation, newborn granule cells migrate from the SGZ outwards in a radial manner into the GCL—termed SGZ and GCL1-3, that is, from the hilus to the molecular layer.[3,45] Interestingly, EGFP + cells that retained high GR expression were located in the internal layers of the GCL, whereas EGFP + cells that showed strong GR knockdown, were consistently located in the more external layers of the GCL (Supplementary Figure 1). Moreover, a marked dispersion of EGFP + cells within the pre-existing GCL was observed 1 week after virus injection, which was absent in control animals (Figures 2a–d). Importantly, a number of these EGFP + cells in the external layers were also positive for BrdU (Supplementary Figure 2), indicating that proliferating newborn cells can migrate relatively fast after GR knockdown. In agreement with previous observations, EGFP + /BrdU + cells were never found in the external layers in control animals.[42,44]

As our observations appeared in line with GC-mediated control of cortical neuron migration during embryonic neurogenesis,[46] we hypothesized that the GR regulates accurate migration of newborn cells within the pre-existing GCL. We therefore compared the positioning of EGFP + within the pre-existing GCL. We found that in GR knockdown animals (Figures 2a–d), the proportion of EGFP + cells located in specific GCL subdivisions was significantly different from control animals (Figure 2e). Strikingly, in GR knockdown animals, a large percentage of the cells had progressed towards the GCL2 and GCL3, whereas 17% of the EGFP + cells were even located in GCL3. In line with normal migration patterns of adult-born new neurons,[42] the majority of the EGFP + cells in control animals were located in the GCL1 and GCL2 (Figure 2e, see also Supplementary Figure 5). Thus, GR knockdown induced an ectopic positioning of a subset of the adult newborn neurons within the existing GCL.

GR knockdown accelerates development of dendritic arborization

Migration during neuronal differentiation is accompanied by changes in the dendritic arborization of DG neurons.[3,45] Cells located in the outer layer show more dendrites that branch from the soma and a more complex dendritic arborization pattern than cells in the inner layer.[47] As GR knockdown increased the number of newborn cells in the more outer layers of the GCL, we wondered whether their dendritic morphology was altered as well. GR knockdown indeed induced different morphological features in individual EGFP + /NeuN + neurons (Figures 3a and b).

Reconstruction of their dendritic morphology revealed two main types of EGFP + neurons to be present within the GCL.[47] One type (Figure 3c) was mainly located in GCL1 and 2, had simpler arbors and generally displayed a unique primary dendrite with a smooth, a spiny proximal dendritic domain and a spiny distal dendritic domain. The other type (Figure 3d) was mostly located in GCL3, had more complex arbors and abundant spines in both its proximal and distal dendritic domains. Sholl analysis confirmed the existence of these two distinct populations of EGFP + neurons within the GCL sublayers (Figure 3e).

To exclude the possibility that these two types of EGFP + neurons were a consequence of different ages of NPCs at the time of lentiviral transduction, we repeated these experiments using retroviral vectors harboring shRNAs against the GR (Supplementary Methods section and Supplementary Figure 9), which allow more precise birthdating.[2] In line with previous studies,[43] we observed EGFP + cells with a simple dendritic arbor, in animals injected with the control shRNA 14 days after retroviral

Figure 1. Glucocorticoid receptor (GR) knockdown regulates neural stem cell (NSC) proliferation and neuronal differentiation. GR is expressed in neuronal nuclei antigen (NeuN) + cells (**a–c**). GR and NeuN are extensively co-expressed in the dentate gyrus (DG; **a**, scale bars: 50 μm; GCL, granule cell layer; H, hilus; ML, molecular layer). Sample orthogonal projections from confocal Z-stack images show that some GR + cells in the subgranulas zone (SGZ) express NeuN (**b**) whereas others do not (**c**). Scale bars in **b**, **c**: 10 μm. GR is expressed in doublecortin (DCX) + cells (**d–h**). The area boxed in **d** is showed in detail in **e** and **f**. Arrows indicate cells that express GR and arrowheads indicate cells that do not express the GR. Sample orthogonal projections from confocal Z-stack images show that some (∼ 50%, H) DCX + cells with morphology resembling type 3 progenitor cells (see also Supplementary Figure 4) express and others do not express the GR (**g, h**; scale bars: 10 μm). Effect of the GR agonist dexamethasone (DEX) on the proliferation of mNSCs in vitro (**i, j**). Cells were incubated with DEX or its vehicle ethanol (control) and stained for the proliferation marker Ki67 (green), and cell nuclei were stained using DAPI (4′,6-diamidino-2-phenylindole; blue). Images show a representative example of three independent experiments performed in triplicates. Scale bars: 20 μm. The dose-dependent effect of DEX on NSC proliferation evaluated by Ki67 expression (**k**). The estimated EC50 value for DEX was 8.24 ± 0.17, in range with previously reported[24] values for GR-mediated actions. Values represent mean ± s.e.m. of three independent experiments performed in triplicates. DEX dose-dependent inhibition of caspase-3 activity in NSCs in vitro (**l**). The estimated EC50 value for DEX was 8.93 ± 0.09. Values represent mean ± s.e.m. of three independent experiments performed in triplicates. Effect of GR knockdown on DEX-induced inhibition of caspase-3 activity in mNSCs in vitro (**m**). Values represent mean ± s.e.m. of three independent experiments performed in triplicates. *P > 0.05 Student's t-test. Effect of increasing doses of small interfering RNA on GR expression (**n**). Values represent mean ± s.e.m. of three independent experiments performed in triplicates. See also Supplementary Figure 7). Sample confocal images corresponding to control (**o, r, u**) and GR knockdown (**p, s, v**) animals 1 week post injection (wpi), showing EGFP and nestin, (**o, p**) EGFP and DCX (**r, s**) and EGFP and NeuN (**u, v**) co-immunostainings. Red hairlines point to cells that co-express the corresponding markers, except in **r**, where the hairlines point to a EGFP + cell in GCL2 that, in contrast to similar ones in GR knockdown animals (hairline in **s**), does not express DCX. All confocal images present one single focal plane where co-localization between the markers of interest is visible. (See also Supplementary Figures 2 and 8 for more details). Scale bars in **o–w**: 10 μm. Distribution plots of EGFP and nestin (**q**), DCX (**t**) and NeuN (**w**) double-positive cells within four sublayers of the GCL (SGZ, GCL1-3, see also Supplementary Figure 5). Results are expressed as percentage of total EGFP + per sublayer. Values represent mean ± s.d. (N = 5 animals per group); *P < 0.05, unpaired Student's t-test. Nestin-positive cells were only observed in the SGZ.
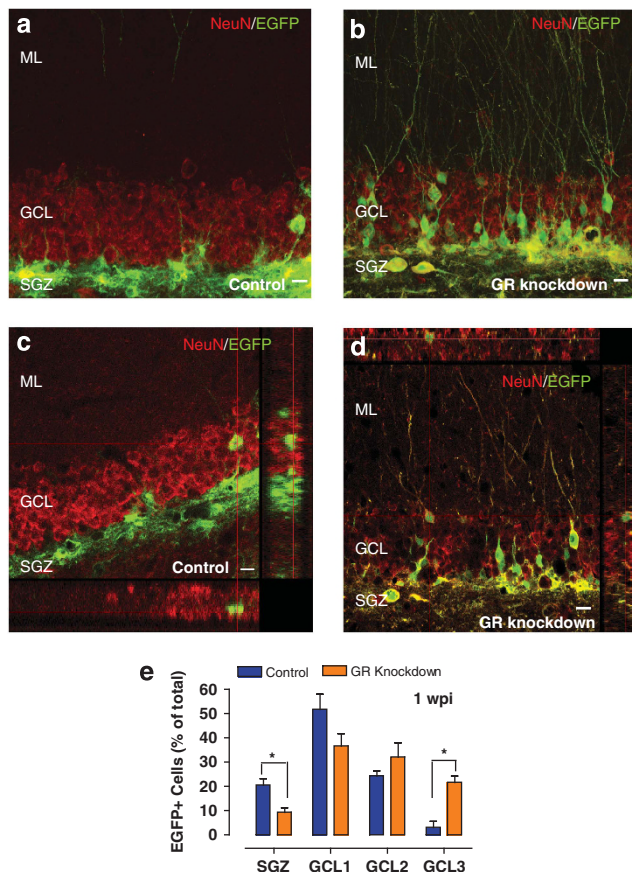
Figure 2. Glucocorticoid receptor (GR) regulates positioning of newborn neurons within the granular cell layer (GCL). Sample confocal images of enhanced green fluorescent protein (EGFP; green) and neuronal nuclei antigen (NeuN; red) immunostainings in control (**a**) or GR knockdown (**b**) animals, showing the differential positioning of EGFP+ neurons within the pre-existing granule neurons of the GCL, 1 week post infection (wpi). Corresponding orthogonal projections (**c**, control; **d**, GR knockdown) showing examples of EGFP+/NeuN+ neurons. (**e**) Distribution plots showing the relative positioning of EGFP+ cells within four sub-divisions of the GCL (subgranular zone (SGZ), GCL1-3, Supplementary Figure 5). Results are expressed as percentage of total EGFP+ cells present in the GCL, 1week post infection (wpi). Scale bars: 10 μm. Values represent mean ± s.d. ($n = 5$ animals per group); *$P < 0.05$, unpaired Student's t-test.

transduction (Figures 3h, j and k). Consistent with our lentiviral data, EGFP+ cells with more complex dendritic trees and with a significant increase in the number of apical dendrites in the proximal dendritic domain were found in animals with retroviral-mediated GR knockdown (Figures 3i, l and m). Moreover, EGFP+ cells in GR knockdown animals had progressed further into the GCL than in control animals (compare Figures 3h and i). Sholl analysis confirmed these morphological differences observed between control and GR knockdown groups (Figures 3n and o).

In addition, in GR knockdown animals, a significantly increased proportion of EGFP+ cells was found with a complex arbor (type 2) located in the GCL3 (Figures 3f and g). All of the EGFP+ cells found in GCL3, both in control and GR knockdown animals, were classifed as type 2, based on their dendritic complexity as assessed by Sholl analysis, whereas type 1 cells were absent from the GCL3 in all animal groups.

The highly similar morphological alterations of individual cells observed after lenti- or retroviral labeling indicates these changes are independent of the viral vector and due to GR knockdown in the immature DG cells. Overall, these observations are consistent with a premature maturation and ectopic positioning of the newborn neurons in the adult hippocampus after GR knockdown.
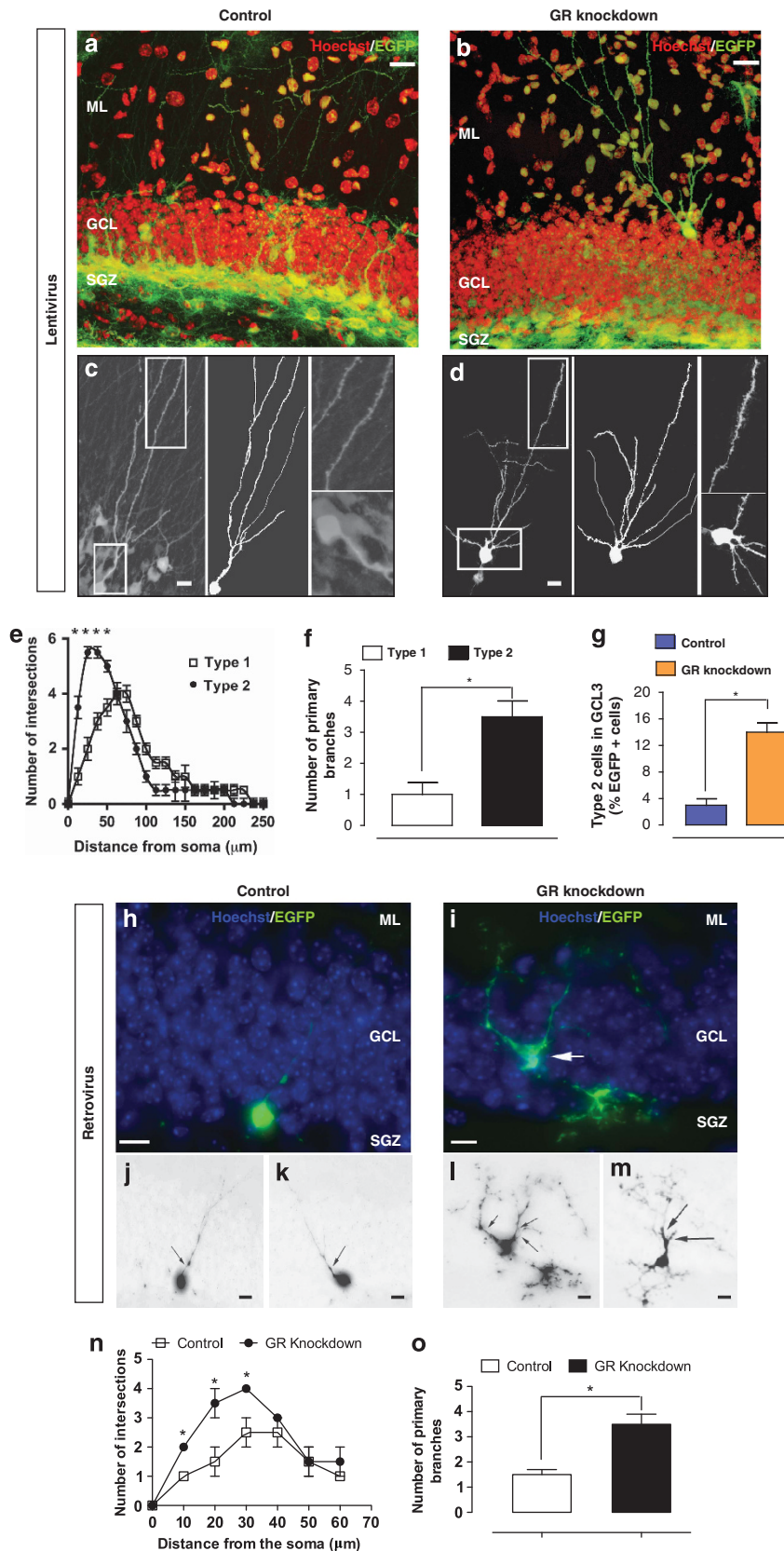
GR knockdown accelerates dendritic spine and bouton maturation of granule cells

We next analyzed EGFP+/NeuN+ neurons and determined the density and shape of the dendritic spines of cells with visible spines in the proximal molecular layer (Figures 4a–e). No significant difference was found in the total spine density between EGFP+/NeuN+ cells in control and GR knockdown animals (Figure 4f). The average spine densities that we found are consistent with spine densities previously observed in young newborn hippocampal neurons of approximately 2 weeks old.[48] Strikingly, a significant increase was present in the percentage of mushroom and thin spines in EGFP+/NeuN+ cells from GR knockdown animals (Figures 4g and h and Supplementary Movies S1 and S2). This increase in mushroom and thin spines was accompanied by a significant decrease in stubby spines in GR knockdown neurons (Figure 4i). Overall, stubby spines were the predominant group of spines (69%) in control animals, whereas in GR knockdown animals, mushroom spines predominated (38%). Interestingly, although thin spines were the minority in GR knockdown cells, they constituted the group with the largest fold-change (Figure 4h). These results are again consistent with an accelerated maturation of newborn neurons after GR knockdown. Moreover, as the size of the spine head can correlate with the

Figure 3. Glucocorticoid receptor (GR) regulates dendritic morphology of newborn neurons. Sample confocal images showing dendritic morphology of enhanced green fluorescent protein (EGFP)+ cells and their location within the granular cell layer (GCL) from control (**a**) or GR knockdown (**b**) groups, using lentiviral vectors. Scale bar: 10 μm. Three-dimensional (3D) confocal reconstruction of somas and dendrites of EGFP+ newborn neurons, obtained 1 week post injection (wpi) with lentiviral vectors (**c**, control; **d**, GR knockdown). Left panels show original images, center panels show corresponding two-dimensional projected dendritic trajectories, and right panels show details of the distal (top) or proximal (bottom) to soma dendritic domains corresponding to boxed areas in the original image. Panels showing proximal domains were rotated 90° clockwise. Only EGFP+ neurons with obvious dendritic spines were considered for analysis. Scale bar: 10 μm. (**e**) Sholl analysis of dendritic complexity of EGFP+ neurons 1 wpi with lentiviral vectors. Values represent mean ± s.d. ($N = 5$ animals per group), *$P < 0.05$, one-way analysis of variance (ANOVA). (**f**) Dendritic properties of EGFP+ newborn neurons 1 wpi. Values represent mean ± s.d. (same cells as in **e**, $N = 5$ animals per group), *$P < 0.05$, unpaired Student's t-test. (**g**) Presence of cells with complex dendritic arbors (type 2) in GCL3 as percentage of total EGFP+ cells in control versus GR knockdown animals. *$P < 0.05$, unpaired Student's t-test. Sample confocal images showing dendritic morphology of EGFP+ cells and their location within the GCL from control (**h**) or GR knockdown (**i**) groups using retroviral vectors. The 3D confocal reconstruction of somas and dendrites of EGFP+ newborn neurons from control (**j**, **k**) or GR knockdown (**l**, **m**) groups, obtained 14 days post injection with retroviral vectors. Only EGFP+ neurons with obvious dendrites projecting to the ML were considered for analysis. Scale bar: 15 μm. Sholl analysis of dendritic complexity of EGFP+ neurons 14 days post injection with retroviral vectors (**n**). Values represent mean ± s.d. ($N = 24$ cells analyzed), *$P < 0.05$, one-way ANOVA. Number of primary branches of retroviral-transduced EGFP+ neurons (**o**). Primary branches were counted in the first 20 μm from the soma. Values in represent mean ± s.e.m. (same cells as in **n**), *$P < 0.05$, unpaired Student's t-test. Arrows in **j–m** point to example cells with single or multiple primary dendrites.

efficacy of the corresponding synapse,[49] our results implicate GR protein levels in controlling synaptic efficacy in the newborn granule neurons of the adult hippocampus.

Recent observations have suggested that maturation of functional input (dendritic spines) and output (axon terminals) of newborn neurons of the hippocampus are synchronized and
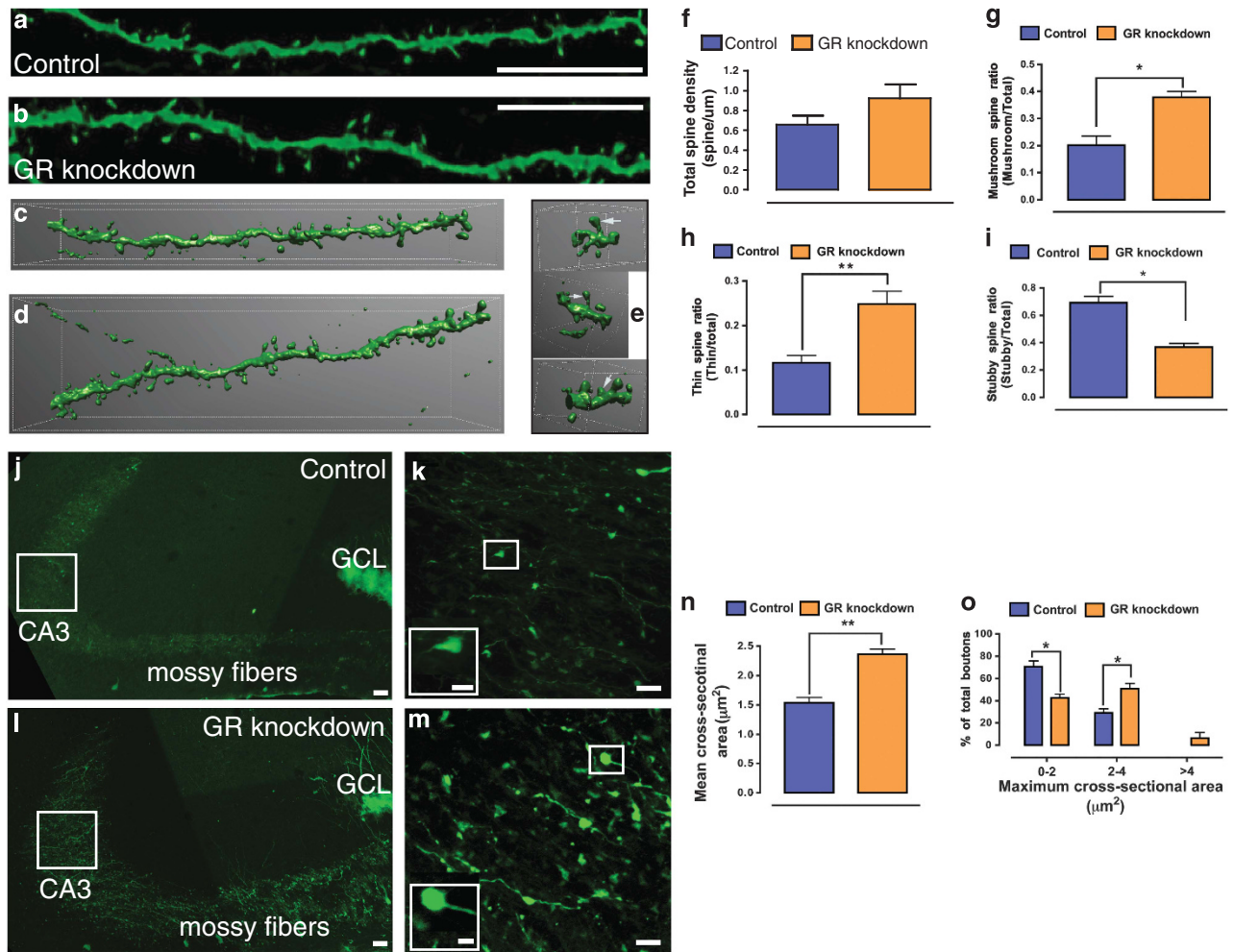
Figure 4. Glucocorticoid receptor (GR) regulates dendritic spine and mossy fiber bouton maturation in newborn neurons. Sample deconvolved confocal images of spiny dendrites of newborn neurons in (**a**) control or (**b**) GR knockdown animals and their corresponding three-dimensional (3D) reconstructions (**c**, control; **d**, GR knockdown). Scale bar: 10 μm. Examples of 3D reconstructions of individual mushroom (**e**, top), thin (**e**, middle) or stubby (**e**, bottom) dendritic spines, indicated by arrows. Spine measurements corresponding to (**f**) total, (**g**) mushroom, (**h**) thin and (**i**) stubby-shaped spines in control versus GR knockdown animals. Values represent mean ± s.d. ($N = 5$ animals per group), *$P < 0.05$, unpaired Student's t-test. See also Supplementary Movies S1 and S2. Sample confocal images showing an overview of the mossy fiber pathway with a subpopulation of lentivirus-transduced axons in green (enhanced green fluorescent protein (EGFP)) in control (**j**) or GR knockdown (**l**) animals, 1 week post injection (wpi). Images are compositions of 3–4 individual images obtained at × 40 magnification and processed using the automatic Photomerge function of Adobe Photoshop CS2 (Macintosh version). Examples of mossy fiber giant boutons labeled with EGFP in the boxed areas in CA3 corresponding to control (**k**) or GR knockdown (**m**) animals. Insets show higher magnification examples of giant boutons in the CA3. Scale bars: 20 (**j, l**), 10 (**k, m**) and 2.5 μm (insets). Mean cross-sectional area of EGFP + boutons at the largest section (**n**), calculated from 3D reconstructions of original images exemplified in **b** and **d** in control versus GR knockdown animals. Frequency distribution plot of the size of giant mossy fiber boutons (**o**) in control versus GR knockdown animals. Giant mossy fiber boutons in CA3 were grouped according to their size, and the percentage of boutons in each size group was calculated. In all cases, values represent mean ± s.d. ($N = 5$ animals per group); *$P < 0.05$, unpaired Student's t-test.

occurs within a discrete time frame, with the cross-sectional area of mossy fiber boutons correlating with age of the newborn cells and reflecting the maturity of the corresponding synapse.[30] Therefore, we studied the cross-sectional area of axon terminals in the CA3 area using confocal microscopy (Figures 4j–m). We found that the mossy fiber boutons in CA3 were substantially larger in 1 week GR knockdown animals than those in the control group animals (Figures 4k and m). The mossy fiber boutons in GR knockdown animals had a significantly larger mean cross-sectional area than those in control animals (Figure 4n, $P < 0.01$). Moreover, a frequency distribution analysis of mossy fiber bouton size showed that in control animals, the majority of the boutons had a cross-sectional area smaller than 2 μm², whereas in GR knockdown animals, the majority of the boutons had a cross-sectional area

larger than 2 μm² (Figure 4o). Together, these results suggest that GR knockdown in adult-born granule cells induces premature cell maturation and consequently a differential pattern of connectivity with the existing hippocampal circuit that may result in increased excitability.

Morphological phenotype persists for at least 5 weeks after GR knockdown

To test the effects of GR knockdown on excitability, and particularly behavior, we selected animals that had recovered for > 1 month after lentiviral delivery. Therefore, we first examined if the morphological features observed 1 week after transduction were still discernable 5 weeks later. First, we analyzed the location
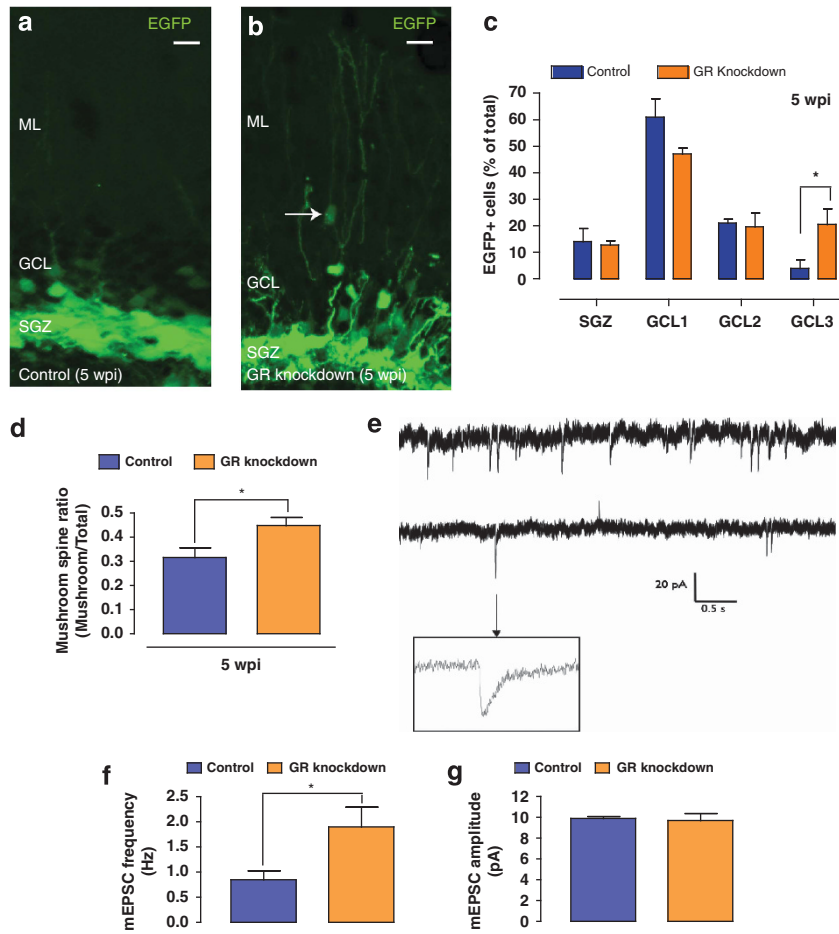
Figure 5. Glucocorticoid receptor (GR) regulates resting membrane electrophysiological properties of newborn neurons. Sample confocal images of enhanced green fluorescent protein (EGFP)+ (green) cells from control (**a**) or GR knockdown (**b**) animals 5 weeks post infection (wpi), showing the persistent mislocation of EGFP+ cells after GR knockdown. The arrow in **b** shows a sample EGFP+ cell ectopically located in the molecular layer (ML). (**c**) Bar graphs showing the relative positioning of EGFP+ cells within four subdivisions of the granular cell layer (GCL; subgranular zone (SGZ), GCL1-3; Supplementary Figure 5) normalized to total EGFP+ cell numbers 5 wpi in control versus GR knockdown animals. Values represent mean ± s.d. ($N = 5$ animals per group); *$P < 0.05$, unpaired Student's t-test. GR knockdown induced a long-lasting effect on dendritic spine maturation. Spine measurements corresponding to (**d**) mushroom-shaped, and (Supplementary Figure 6) thin and stubby-shaped spines in control versus GR knockdown animals. Values represent mean ± s.d. ($N = 5$ animals per group), *$P < 0.05$, unpaired Student's t-test. (**e**) Examples of typical miniature excitatory postsynaptic current (mEPSC) recordings in granule cells from GR knockdown animals (top) or controls (bottom), 5 wpi. Inset shows a sample mEPSC. Scale bars represent 0.5 s, 20 pA. On average, mEPSC frequency (**f**) but not amplitude (**g**) was enhanced in granule cells from GR knockdown versus control animals. Values represent mean ± s.e.m.: $N = 10$ cells per group (one to two cells per animal); *$P < 0.05$, unpaired Student's t-test.

of EGFP+ cells within the GCL to check whether the ectopic location of the newborn cells after GR knockdown persisted 5 weeks after injection. Similar to the 1 week time point, significantly ($P < 0.01$) higher numbers of EGFP+ cells were found in GCL3 in GR knockdown animals compared with control animals, with some cells being ectopically located in the molecular layer (Figures 5a–c).

These long-lasting effects of GR knockdown on new cell positioning were also evident from the density and shape of the dendritic spines from EGFP+/NeuN+ neurons (Figure 5d). At this 5-week time point, the average total spine densities found in control animals was consistent with spine densities previously observed in young newborn hippocampal neurons of approximately 1 month old[48,50] (Supplementary Figure 10). Comparable to what was observed 1 week after injection, we found no significant differences in total spine density between EGFP+/NeuN+ cells in control or GR knockdown animals at the later time point (Supplementary Figure 10). Importantly, and again consistent with the results observed 1 week after LV injection, we also

found a significant increase in the percentage of mushroom (Figure 5d) and thin spines at 5 weeks after injection, which was accompanied by a significant decrease in stubby spines (Supplementary Figure 10) in the EGFP+/NeuN+ cells from GR knockdown animals.

GR knockdown promotes spontaneous excitatory synaptic events of granule cells

To measure excitatory transmission in newborn neurons 5 weeks after GR knockdown compared with control, we used whole cell voltage clamp (holding potential $V_H = -70$ mV) to record mEPSCs (Figure 5e), each reflecting the spontaneous release of a single glutamate-containing vesicle. EGFP+ cells within the granule cell layer were identified as granule cells by the shape and location of their soma and dendritic tree. Consistent with the increased proportion of mature spines, EGFP+ cells in GR knockdown animals presented a significant ($P = 0.03$) increase in the frequency of mEPSCs compared with EGFP+ cells in control

animals (Figure 5f). The mean frequency of mEPSCs in control EGFP + cells was highly comparable to that of neighboring non-EGFP + cells (data not shown). No differences in mEPSC amplitude were detected between GR knockdown and control EGFP + cells (Figure 5g) or neighboring EGFP$^+$ cells. Collectively, these data corroborate that GR knockdown in newborn granule neurons induces drastic increases in spontaneous glutamate-receptor-mediated transmission.

GR knockdown in newborn neurons of the hippocampus impairs memory consolidation

Four weeks after birth, newborn neurons are considered to be fully integrated into the hippocampal network and participate in hippocampal tasks.[51] To address the behavioral consequences of the altered morphology and aberrant positioning of the newborn neurons and their increased mEPSC frequency after GR knockdown, we analyzed hippocampus-dependent contextual learning 5 weeks after virus injection.

As several studies have shown a relationship between adult neurogenesis and contextual fear conditioning in rodents,[4,52] we measured freezing behavior in groups of GR knockdown and control animals[32] (Figure 6a). On day 1, GR knockdown and control animals exhibited similar freezing behavior in both the context and cue test, suggesting that task acquisition was not affected by GR knockdown (Figures 6b and c). Interestingly, on day 2, a significant ($P < 0.01$) reduction in context-induced freezing time was present in GR knockdown animals, whereas cue-induced freezing time was unaffected (Figures 6d and e). The reduction in freezing was most obvious in the first trials on day 2, indicating that particularly memory consolidation is impaired. Also on day 3, a significantly ($P < 0.05$) reduced contextual, but not cued, freezing time was evident in the GR knockdown animals (Figures 6f and g). Together, this suggests that particularly context-dependent memory consolidation, but not cue-dependent memory consolidation, was impaired after GR knockdown in newborn DG cells.

To control for possible effects of GR knockdown on circulating levels of corticosterone, basal morning and evening plasma concentrations were measured 1 day before the memory acquisition phase of the fear-conditioning protocol, and 30 and 60 min after the conditioning protocol on days 1 to 3 (Figure 6a). As previously described,[32] plasma corticosterone levels immediately after fear conditioning were significantly higher than the basal levels measured the day before (Supplementary Figure 11). Although no differences were observed between GR knockdown and control animals in circulating basal corticosterone levels, the elevated levels have been high enough to activate the GR during the fear conditioning (Supplementary Figure 11). Together, this supports the notion that the behavioral differences are due to downregulation of the GR in the cells of the hippocampal neurogenic niche.

DISCUSSION

We have demonstrated that GR protein levels influence the structural and functional integration of the individual newborn cells into the adult hippocampal network. GR knockdown altered their relative positioning in the GCL and promoted their placement in more external layers. In parallel, GR knockdown accelerated neuronal maturation and altered spine morphology of the individual newborn cells that showed relatively more mature thin and mushroom spines, and less immature stubby spines. In functional terms, neurons with GR knockdown exhibited an increased basal neuronal activity, whereas GR knockdown animals showed a significant impairment in hippocampus—but not hippocampus-independent—memory.

Although several studies had already indicated that aberrant GC signaling impairs proliferation, maturation and/or survival of NPCs
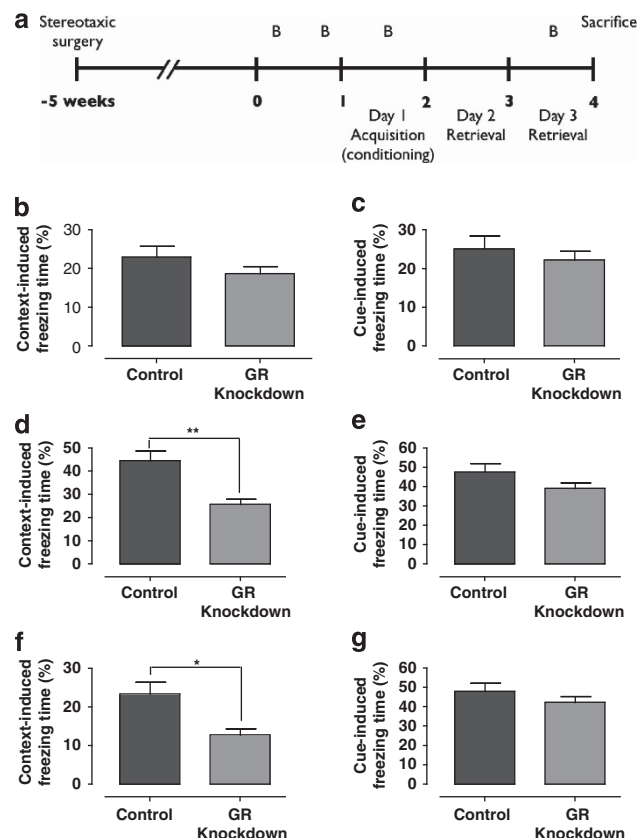

Figure 6. Glucocorticoid receptor (GR) is involved in hippocampal memory consolidation. Scheme showing the design of the fear-conditioning experiments performed with control and GR knockdown animals (**a**). The letter B in the schematic protocol represents blood extraction for corticosterone measurements. Bar graphs showing context induced (left) and cue-induced (right) freezing time values in control versus GR knockdown animals in the first day (**b, c**), second day (**d, e**) and third day (**f, g**) of the fear-conditioning protocol. Values represent mean ± s.e.m., $N = 40$ animals per group; *$P < 0.05$, **$P < 0.01$, unpaired Student's t-test.

in the adult DG (see for example, Wong et al.[34]), the precise role of the GR in the regulation of neurogenesis in the SGZ remained elusive. As virtually every cell type in the DG expresses GR, studies that targeted GR in defined cell types using classical transgenic approaches were difficult to interpret. Therefore, we used lentiviral and retroviral vectors in vivo to knockdown GR selectively in cells of the hippocampus neurogenic niche only,[27] to investigate the cellular, functional and behavioral consequences. Our data clearly demonstrate that GR knockdown directly affects the position, fate and function of the adult-generated neurons and thereby disturbs hippocampus-dependent memory consolidation.

As a very small minority of the transduced cells was positive for mature neuronal markers 1 week after LV injection,[27] we cannot completely exclude the possibility that GR knockdown in these few mature cells may have contributed, at least in part, to the present results. Also a very small percentage of the EGFP$^+$ cells was located in the hilus, that may represent astrocytes or mossy cells/hilar interneurons, populations known to express GR.[22,53] However, given the high number of transduced cells located in the GCL and SGZ, and their scarcity in the hilar regions, we favor the view that the observed effects are due to GR knockdown in the immature, adult-born granule cells.

As GCs also activate MR and GR/MR heterodimers,[54] GR knockdown could have resulted in a preferential activation of

MRs. This situation is known to trigger a genetic pro-survival program in hippocampal neurons[55] that restrains proliferation and apoptosis.[56] Although this, at least in theory, might have been involved in the accelerated neuronal differentiation, there are several arguments to support that our findings are specifically explained by GR knockdown rather than by indirect effects via MR.

First, as shown before,[27] the majority of the cells (>85%) targeted by our lentiviral vector are positive for immature neural cell markers. These immature cells do express GR, but so far, MR expression was below detection level.[22] Second, we did not observe changes in MR expression in the mature cells of the GCL after GR knockdown, indicating the absence of a compensatory mechanisms at the level of MR. Nevertheless, we cannot entirely exclude the possibility that, particularly, the effects on basal excitability and the effects on memory consolidation are, at least partly, mediated by an increased MR/GR ratio in the few mature cells, which were subject to GR knockdown.

A third argument comes from studies in adrenalectomized (ADX) animals; instead of exposing animals to high GC levels sufficient to activate both MR and GR, and then altering GR expression, exposure of rodents to very low GC levels will preferentially activate MRs but not GRs. ADX in rats is well known to increase proliferation of progenitor cells.[5,6,57,58] Adrenalectomy of rats resulted in dentate granule cells with a relatively simple dendritic arborization, yielding overall reduced dendritic length. Yet, rats with residual levels of corticosterone after ADX—causing almost exclusive MR activation—displayed complex dendritic trees with an arborization pattern and dendritic length resembling that of the presumably mature cells located in the outer granule cell layer of sham-operated controls.[59]

In view of possible species differences, we also carried out a pilot study to examine effects of ADX on NPC proliferation and granule cell morphology. In mice, ADX is known to remove most but not all corticosterone, due to residual corticosteroid levels produced in accessory fat cells.[60,61] In line with what was described in rats with an incomplete removal of corticosterone, we found that newborn cells located in GCL2 and 3 had multiple primary dendrites that were not present in SHAM-operated mice (Supplementary Figure 12). Also, the number of DCX$^+$ cells after ADX was on average significantly higher than in SHAM-operated controls, particularly in GCL1 (Supplementary Figure 12).

These data suggest that in two approaches in which GR activation was strongly reduced, a highly comparable morphological phenotype was observed. This supports the critical importance of GRs in (containing the) maturation of newborn cells. It further extends earlier work by emphasizing the key role of GRs particularly expressed in the NPCs rather than in other, more mature DG cells. GRs in the NPCs thus may direct the positioning of newborn granule cells into the pre-existing granule cell layer. In addition to cell-intrinsic factors, cell-extrinsic factors are involved in this process and in the integration of newborn cells, some of which have been identified.[45] We observed an increased proportion of cells with a complex dendritic arbor in the GCL3 of GR knockdown animals. This observation suggests that the accelerated maturation and morphological alterations could be a result of the relative cellular positioning within the GCL observed after GR knockdown, rather than enhanced speed of maturation. Although similar morphological alterations in dendritic arborization were observed using retroviral vectors, the mislocation phenotype was milder. Therefore, morphological alterations in dendritic arborization may be independent of cellular mislocation induced by GR knockdown. The most likely explanation seems that GR knockdown has increased the maturation speed of young immature cell in the DG. However, we can not exclude at this point that the severity of the positioning phenotype could reflect different degrees of GR knockdown achieved in vivo with different viruses.

The altered differentiation and maturation of newborn granule cells after GR knockdown, and the concomitant increase in basal membrane excitability, correlated with impaired contextual memory consolidation, is consistent with several recent studies (reviewed in Deng et al.[4]). The majority of these studies aimed to physically or genetically impair the rate of neurogenesis, whereas our study focused on maturation, and particularly the relative positioning of the newborn cells and their functional relevance. One alternative explanation for the impaired contextual memory consolidation may be that GR function was reduced in newborn cells, regardless of the position of the cells. Indeed, loss of GR function by ADX or pharmacological inhibition of GR activity has been shown to also impair memory consolidation for contextual fear conditioning in rats.[62]

Loss of GR function, though, does not seem to be a prerequisite for an aberrant placement of DG cells that in turn, may affect hippocampus-dependent memory tasks. For instance, knockdown of disrupted-in-schizophrenia 1 (DISC1) in cells of the hippocampus neurogenic niche causes strikingly similar effects to those observed after GR knockdown, including an accelerated neuronal maturation and changes in synapse formation, and also aberrant integration of newborn cells into hippocampal networks.[45] Local DISC1 knockdown in the DG also resulted in impaired performances of mice in several hippocampus-dependent tasks.[63] Similarly, phospholipase-Cβ1 knockout mice exhibit a comparable misposi-tioning of adult newborn cells to more outer layers, and these mice are also impaired in hippocampus-dependent memory consoli-dation.[64] However, a possible link between GR-activated signaling pathways, DISC1 or phospholipase-Cβ1 is at present unknown, and the observed phenotypic overlap might also be caused by independent pathways.

Overall, our data indicate that GR protein levels, and thereby GR activation in the newborn granule cells, should be within a narrow window of expression, with low expression levels being beneficial for neuronal maturation of newborn cells, and relatively high expression levels may have pathological consequences for neuronal integrity and hence hippocampus-dependent functions. GR expression itself is regulated a.o. by endogenous factors and recently, we have shown that GR protein levels are downregulated by microRNA-124,[26] a non-coding, endogenous RNA that is highly expressed in, and specific for, neuronal cells. Interestingly, recent in vivo experiments have identified microRNA-124 as a 'master switch' that turns on a neuronal differentiation program in neuronal progenitor cells.[25] This suggests that restriction of GR activity may be necessary to allow neuronal differentiation of NPCs, a notion that is well in line with our data.

Conversely, GR levels should not be too low. Several risk factors for the pathogenesis of psychiatric disorders have been shown to result in reduced GR protein levels. For instance, early life stress in rats as well as chronic stress exposure in adulthood are well-known risk factors for psychopathology, and reduce GR protein and/or mRNA levels in the hippocampus.[65] Also, aging impairs the negative feedback of GCs on the hypothalamic–pituitary–adrenal axis, which leads to elevated GC levels, reduced GR expression levels[66,67] and reductions in neurogenesis that are associated with decline in cognitive functions.[68] Interestingly, the rate of hippocampal neurogenesis seems positively correlated with improved memory performances in old animals and fluctuating GC may affect such performances by regulating the number of newborn cells.[68,69]

Recent observations have further demonstrated that type 3 cells and comparable neuroblast phenotypes are particularly involved in the impairments in neurogenesis associated with aging.[70] Therefore, extrapolation of these and our present data indicates that reduced GR protein levels may impair hippocampus-dependent memory consolidation by re-organizing hippocampal networks in which newborn cells are involved.

In conclusion, we have demonstrated that endogenous GR expression levels interfere with the migration, morphology,

differentiation and functional integration of individual adult-generated granule cells into the adult hippocampal network. As GR is activated by endogenous ligands like GCs, and is also an important target for pharmacological steroid-based drugs, our data suggest that these compounds can affect correct integration of newborn cells and potentially modulate hippocampus-dependent aspects of cognition common to several psychiatric disorders.

CONFLICT OF INTEREST

The authors declare no conflict of interest.

REFERENCES

1 Gould E, Tanapat P. Stress and hippocampal neurogenesis. *Biol Psychiatry* 1999; **46**: 1472–1479.

2 van Praag H, Schinder AF, Christie BR, Toni N, Palmer TD, Gage FH. Functional neurogenesis in the adult hippocampus. *Nature* 2002; **415**: 1030–1034.

3 Zhao C, Deng W, Gage FH. Mechanisms and functional implications of adult neurogenesis. *Cell* 2008; **132**: 645–660.

4 Deng W, Aimone JB, Gage FH. New neurons and new memories: how does adult hippocampal neurogenesis affect learning and memory? *Nat Rev Neurosci* 2010; **11**: 339–350.

5 Cameron HA, Gould E. Adult neurogenesis is regulated by adrenal steroids in the dentate gyrus. *Neuroscience* 1994; **61**: 203–209.

6 Lucassen PJ, Meerlo P, Naylor AS, van Dam AM, Dayer AG, Fuchs E *et al.* Regulation of adult neurogenesis by stress, sleep disruption, exercise and inflammation: Implications for depression and antidepressant action. *Eur Neuropsychopharmacol* 2010; **20**: 1–17.

7 Yu S, Patchev AV, Wu Y, Lu J, Holsboer F, Zhang JZ *et al.* Depletion of the neural precursor cell pool by glucocorticoids. *Ann Neurol* 2010; **67**: 21–30.

8 Oomen CA, Mayer JL, de Kloet ER, Joels M, Lucassen PJ. Brief treatment with the glucocorticoid receptor antagonist mifepristone normalizes the reduction in neurogenesis after chronic stress. *Eur J Neurosci* 2007; **26**: 3395–3401.

9 Schloesser RJ, Lehmann M, Martinowich K, Manji HK, Herkenham M. Environmental enrichment requires adult neurogenesis to facilitate the recovery from psychosocial stress. *Mol Psychiatry* 2010; **15**: 1152–1163.

10 Wolf SA, Steiner B, Wengner A, Lipp M, Kammertoens T, Kempermann G. Adaptive peripheral immune response increases proliferation of neural precursor cells in the adult hippocampus. *FASEB J* 2009; **23**: 3121–3128.

11 Revest JM, Di Blasi F, Kitchener P, Rouge-Pont F, Desmedt A, Turiault M *et al.* The MAPK pathway and Egr-1 mediate stress-related behavioral effects of glucocorticoids. *Nat Neurosci* 2005; **8**: 664–672.

12 Revest JM, Kaouane N, Mondin M, Le Roux A, Rouge-Pont F, Vallee M *et al.* The enhancement of stress-related memory by glucocorticoids depends on synapsin-Ia/Ib. *Mol Psychiatry* 2010; **15**: 1125, 1140–1151.

13 Gould E, McEwen BS, Tanapat P, Galea LA, Fuchs E. Neurogenesis in the dentate gyrus of the adult tree shrew is regulated by psychosocial stress and NMDA receptor activation. *J Neurosci* 1997; **17**: 2492–2498.

14 Datson NA, Morsink MC, Meijer OC, de Kloet ER. Central corticosteroid actions: Search for gene targets. *Eur J Pharmacol* 2008; **583**: 272–289.

15 Fitzsimons CP, van Hooijdonk LW, Morrow JA, Peeters BW, Hamilton N, Craighead M *et al.* Antiglucocorticoids, neurogenesis and depression. *Mini Rev Med Chem* 2009; **9**: 249–264.

16 Mayer JL, Klumpers L, Maslam S, de Kloet ER, Joels M, Lucassen PJ. Brief treatment with the glucocorticoid receptor antagonist mifepristone normalises the corticosterone-induced reduction of adult hippocampal neurogenesis. *J Neuroendocrinol* 2006; **18**: 629–631.

17 de Kloet ER, Sibug RM, Helmerhorst FM, Schmidt MV. Stress genes and the mechanism of programming the brain for later life. *Neurosci Biobehav Rev* 2005; **29**: 271–281.

18 Holsboer F. The corticosteroid receptor hypothesis of depression. *Neuropsychopharmacology* 2000; **23**: 477–501.

19 Kronenberg G, Kirste I, Inta D, Chourbaji S, Heuser I, Endres M *et al.* Reduced hippocampal neurogenesis in the GR(+/-) genetic mouse model of depression. *Eur Arch Psychiatry Clin Neurosci* 2009; **259**: 499–504.

20 Ridder S, Chourbaji S, Hellweg R, Urani A, Zacher C, Schmid W *et al.* Mice with genetically altered glucocorticoid receptor expression show altered sensitivity for stress-induced depressive reactions. *J Neurosci* 2005; **25**: 6243–6250.

21 Boku S, Nakagawa S, Masuda T, Nishikawa H, Kato A, Kitaichi Y *et al.* Glucocorticoids and lithium reciprocally regulate the proliferation of adult dentate gyrus-derived neural precursor cells through GSK-3beta and beta-catenin/TCF pathway. *Neuropsychopharmacology* 2009; **34**: 805–815.

22 Garcia A, Steiner B, Kronenberg G, Bick-Sander A, Kempermann G. Age-dependent expression of glucocorticoid- and mineralocorticoid receptors on neural precursor cell populations in the adult murine hippocampus. *Aging Cell* 2004; **3**: 363–371.

23 Vreugdenhil E, Kolk SM, Boekhoorn K, Fitzsimons CP, Schaaf M, Schouten T *et al.* Doublecortin-like, a microtubule-associated protein expressed in radial glia, is crucial for neuronal precursor division and radial process stability. *Eur J Neurosci* 2007; **25**: 635–648.

24 Fitzsimons CP, Ahmed S, Wittevrongel CF, Schouten TG, Dijkmans TF, Scheenen WJ *et al.* The microtubule-associated protein doublecortin-like regulates the transport of the glucocorticoid receptor in neuronal progenitor cells. *Mol Endocrinol* 2008; **22**: 248–262.

25 Cheng LC, Pastrana E, Tavazoie M, Doetsch F. miR-124 regulates adult neurogenesis in the subventricular zone stem cell niche. *Nat Neurosci* 2009; **12**: 399–408.

26 Vreugdenhil E, Verissimo CS, Mariman R, Kamphorst JT, Barbosa JS, Zweers T *et al.* MicroRNA 18 and 124a down-regulate the glucocorticoid receptor: implications for glucocorticoid responsiveness in the brain. *Endocrinology* 2009; **150**: 2220–2228.

27 van Hooijdonk LW, Ichwan M, Dijkmans TF, Schouten TG, de Backer MW, Adan RA *et al.* Lentivirus-mediated transgene delivery to the hippocampus reveals sub-field specific differences in expression. *BMC Neurosci* 2009; **10**: 2.

28 Sarabdjitsingh RA, Meijer OC, Schaaf MJ, de Kloet ER. Subregion-specific differences in translocation patterns of mineralocorticoid and glucocorticoid receptors in rat hippocampus. *Brain Res* 2009; **1249**: 43–53.

29 Rodriguez A, Ehlenberger DB, Dickstein DL, Hof PR, Wearne SL. Automated three-dimensional detection and shape classification of dendritic spines from fluorescence microscopy images. *PLoS One* 2008; **3**: e1997.

30 Toni N, Laplagne DA, Zhao C, Lombardi G, Ribak CE, Gage FH *et al.* Neurons born in the adult dentate gyrus form functional synapses with target cells. *Nat Neurosci* 2008; **11**: 901–907.

31 Olijslagers JE, de Kloet ER, Elgersma Y, van Woerden GM, Joels M, Karst H. Rapid changes in hippocampal CA1 pyramidal cell function via pre- as well as postsynaptic membrane mineralocorticoid receptors. *Eur J Neurosci* 2008; **27**: 2542–2550.

32 Brinks V, Berger S, Gass P, de Kloet ER, Oitzl MS. Mineralocorticoid receptors in control of emotional arousal and fear memory. *Horm Behav* 2009; **56**: 232–238.

33 Brown JP, Couillard-Despres S, Cooper-Kuhn CM, Winkler J, Aigner L, Kuhn HG. Transient expression of doublecortin during adult neurogenesis. *J Comp Neurol* 2003; **467**: 1–10.

34 Wong EY, Herbert J. Raised circulating corticosterone inhibits neuronal differentiation of progenitor cells in the adult hippocampus. *Neuroscience* 2006; **137**: 83–92.

35 Cameron HA, Tanapat P, Gould E. Adrenal steroids and N-methyl-D-aspartate receptor activation regulate neurogenesis in the dentate gyrus of adult rats through a common pathway. *Neuroscience* 1998; **82**: 349–354.

36 Anacker C, Zunszain PA, Cattaneo A, Carvalho LA, Garabedian MJ, Thuret S *et al.* Antidepressants increase human hippocampal neurogenesis by activating the glucocorticoid receptor. *Mol Psychiatry* 2011; **16**: 738–750.

37 Garza JC, Guo M, Zhang W, Lu XY. Leptin restores adult hippocampal neurogenesis in a chronic unpredictable stress model of depression and reverses glucocorticoid-induced inhibition of GSK-3beta/beta-catenin signalling. *Mol Psychiatry* 2012; **17**: 790–808.

38 Shuto M, Higuchi K, Sugiyama C, Yoneyama M, Kuramoto N, Nagashima R *et al.* Endogenous and exogenous glucocorticoids prevent trimethyltin from causing neuronal degeneration of the mouse brain *in vivo*: involvement of oxidative stress pathways. *J Pharmacol Sci* 2009; **110**: 424–436.

39 Fernando P, Brunette S, Megeney LA. Neural stem cell differentiation is dependent upon endogenous caspase 3 activity. *FASEB J* 2005; **19**: 1671–1673.

40 Belmokhtar CA, Hillion J, Segal-Bendirdjian E. Staurosporine induces apoptosis through both caspase-dependent and caspase-independent mechanisms. *Oncogene* 2001; **20**: 3354–3362.

41 LoPresti P, Poluha W, Poluha DK, Drinkwater E, Ross AH. Neuronal differentiation triggered by blocking cell proliferation. *Cell Growth Differ* 1992; **3**: 627–635.

42 Kempermann G, Gast D, Kronenberg G, Yamaguchi M, Gage FH. Early determination and long-term persistence of adult-generated new neurons in the hippocampus of mice. *Development* 2003; **130**: 391–399.

43 Esposito MS, Piatti VC, Laplagne DA, Morgenstern NA, Ferrari CC, Pitossi FJ et al. Neuronal differentiation in the adult hippocampus recapitulates embryonic development. J Neurosci 2005; 25: 10074–10086.

44 Mathews EA, Morgenstern NA, Piatti VC, Zhao C, Jessberger S, Schinder AF et al. A distinctive layering pattern of mouse dentate granule cells is generated by developmental and adult neurogenesis. J Comp Neurol 2010; 518: 4479–4490.

45 Duan X, Chang JH, Ge S, Faulkner RL, Kim JY, Kitabatake Y et al. Disrupted-In-Schizophrenia 1 regulates integration of newly generated neurons in the adult brain. Cell 2007; 130: 1146–1158.

46 Fukumoto K, Morita T, Mayanagi T, Tanokashira D, Yoshida T, Sakai A et al. Detrimental effects of glucocorticoids on neuronal migration during brain development. Mol Psychiatry 2009; 14: 1119–1131.

47 Redila VA, Christie BR. Exercise-induced changes in dendritic structure and complexity in the adult hippocampal dentate gyrus. Neuroscience 2006; 137: 1299–1307.

48 Zhao C, Teng EM, Summers Jr RG , Ming GL, Gage FH. Distinct morphological stages of dentate granule neuron maturation in the adult mouse hippocampus. J Neurosci 2006; 26: 3–11.

49 Bourne JN, Harris KM. Balancing structure and function at hippocampal dendritic spines. Annu Rev Neurosci 2008; 31: 47–67.

50 Toni N, Teng EM, Bushong EA, Aimone JB, Zhao C, Consiglio A et al. Synapse formation on neurons born in the adult hippocampus. Nat Neurosci 2007; 10: 727–734.

51 Kee N, Teixeira CM, Wang AH, Frankland PW. Preferential incorporation of adult-generated granule cells into spatial memory networks in the dentate gyrus. Nat Neurosci 2007; 10: 355–362.

52 Kirby ED, Friedman AR, Covarrubias D, Ying C, Sun WG, Goosens KA et al. Basolateral amygdala regulation of adult hippocampal neurogenesis and fear-related activation of newborn neurons. Mol Psychiatry 2012; 17: 527–536.

53 Hu W, Zhang M, Czeh B, Flugge G, Zhang W. Stress impairs GABAergic network function in the hippocampus by activating nongenomic glucocorticoid receptors and affecting the integrity of the parvalbumin-expressing neuronal network. Neuropsychopharmacology 2010; 35: 1693–1707.

54 Trapp T, Rupprecht R, Castren M, Reul JM, Holsboer F. Heterodimerization between mineralocorticoid and glucocorticoid receptor: a new principle of glucocorticoid action in the CNS. Neuron 1994; 13: 1457–1462.

55 Almeida OF, Conde GL, Crochemore C, Demeneix BA, Fischer D, Hassan AH et al. Subtle shifts in the ratio between pro- and antiapoptotic molecules after activation of corticosteroid receptors decide neuronal fate. FASEB J 2000; 14: 779–790.

56 Hu Z, Yuri K, Ozawa H, Lu H, Kawata M. The in vivo time course for elimination of adrenalectomy-induced apoptotic profiles from the granule cell layer of the rat hippocampus. J Neurosci 1997; 17: 3981–3989.

57 Montaron MF, Piazza PV, Aurousseau C, Urani A, Le Moal M, Abrous DN. Implication of corticosteroid receptors in the regulation of hippocampal structural plasticity. Eur J Neurosci 2003; 18: 3105–3111.

58 Wong EY, Herbert J. Roles of mineralocorticoid and glucocorticoid receptors in the regulation of progenitor proliferation in the adult hippocampus. Eur J Neurosci 2005; 22: 785–792.

59 Wossink J, Karst H, Mayboroda O, Joels M. Morphological and functional properties of rat dentate granule cells after adrenalectomy. Neuroscience 2001; 108: 263–272.

60 Brinks V, van der Mark MH, de Kloet ER, Oitzl MS. Differential MR/GR activation in mice results in emotional states beneficial or impairing for cognition. Neural Plast 2007 90163.

61 Jacobson L. Glucocorticoid replacement, but not corticotropin-releasing hormone deficiency, prevents adrenalectomy-induced anorexia in mice. Endocrinology 1999; 140: 310–317.

62 Sandi C, Merino JJ, Cordero MI, Touyarot K, Venero C. Effects of chronic stress on contextual fear conditioning and the hippocampal expression of the neural cell adhesion molecule, its polysialylation, and L1. Neuroscience 2001; 102: 329–339.

63 Mao Y, Ge X, Frank CL, Madison JM, Koehler AN, Doud MK et al. Disrupted in schizophrenia 1 regulates neuronal progenitor proliferation via modulation of GSK3beta/beta-catenin signaling. Cell 2009; 136: 1017–1031.

64 Manning EE, Ransome MI, Burrows EL, Hannan AJ. Increased adult hippocampal neurogenesis and abnormal migration of adult-born granule neurons is associated with hippocampal-specific cognitive deficits in phospholipase C-beta1 knockout mice. Hippocampus 2010; 22: 309–319.

65 Weaver IC, Cervoni N, Champagne FA, D'Alessio AC, Sharma S, Seckl JR et al. Epigenetic programming by maternal behavior. Nat Neurosci 2004; 7: 847–854.

66 Mizoguchi K, Ikeda R, Shoji H, Tanaka Y, Maruyama W, Tabira T. Aging attenuates glucocorticoid negative feedback in rat brain. Neuroscience 2009; 159: 259–270.

67 Murphy EK, Spencer RL, Sipe KJ, Herman JP. Decrements in nuclear glucocorticoid receptor (GR) protein levels and DNA binding in aged rat hippocampus. Endocrinology 2002; 143: 1362–1370.

68 Abrous DN, Koehl M, Le Moal M. Adult neurogenesis: from precursors to network and physiology. Physiol Rev 2005; 85: 523–569.

69 Montaron MF, Drapeau E, Dupret D, Kitchener P, Aurousseau C, Le Moal M et al. Lifelong corticosterone level determines age-related decline in neurogenesis and memory. Neurobiol Aging 2006; 27: 645–654.

70 Lugert S, Basak O, Knuckles P, Haussler U, Fabel K, Gotz M et al. Quiescent and active hippocampal neural stem cells with distinct morphologies respond selectively to physiological and pathological stimuli and aging. Cell Stem Cell 2010; 6: 445–456.